Neodymium recovery from scrap magnet using ammonium persulfate

Erwin Ciro, Andrea Alzate, Esperanza López, Claudia Serna, Oberlando Gonzalez

PII: S0304-386X(18)30345-1
DOI: https://doi.org/10.1016/j.hydromet.2019.04.016
Reference: HYDROM 5043

To appear in: *Hydrometallurgy*

Received date: 9 May 2018
Revised date: 28 March 2019
Accepted date: 9 April 2019

Please cite this article as: E. Ciro, A. Alzate, E. López, et al., Neodymium recovery from scrap magnet using ammonium persulfate, Hydrometallurgy, https://doi.org/10.1016/j.hydromet.2019.04.016

Neodymium recovery from scrap magnet using ammonium persulfate

Erwin Ciro[a], Andrea Alzate[a*], Esperanza López[a], Claudia Serna[a], Oberlando Gonzalez[b]

[a] *GIPIMME Research Group, Department of Materials Engineering, University of Antioquia, CL 67 53-108, Medellín-Colombia*
[b] *ALTERO S.A.S, CL 28 75-32 Medellín-Colombia*
** Corresponding author. GIPIMME Research Group, University of Antioquia, Cl 67 53-108, Medellin-Colombia, e-mail address: andreaalzatenaranjo@gmail.com, erwinciro@gmail.com*

ABSTRACT:

This study proposes a novel leaching methodology to recover neodymium from scrap magnet using ammonium persulfate ($(NH_4)_2S_2O_8$) solutions. The Nd–Fe–B magnets from obsolete Hard-Disk-Drives were physically treated by thermal demagnetization (400 °C, 45 min) and mechanical crushing (< 420 µm). The chemical composition of the ground sample was Nd: 31.5 wt%, Fe: 64.8 wt%, Co: 1.9 wt%, Ni: 0.6 wt%. Diagrams of equilibrium phases (Eh vs. pH) were designed to determine the predominance of the formed species in the $(NH_4)_2S_2O_8$ system. Ammonium persulfate aqueous solutions were prepared to generate oxidative sulfate radicals. These radicals allowed to leach the ground samples of Nd–Fe–B magnets and recover of neodymium sulfate. The influence of $(NH_4)_2S_2O_8$ concentration (0.7 – 1.3 M), temperature (25 – 75 °C) and L/S ratio (25 – 50 mL/g) on Nd–Fe–B magnets leaching was investigated employing analysis of variance in a 2^3 full factorial experimental design. At the optimal conditions, quantities greater than 98% of Nd–Fe–B magnets were leached after 15 min reaction time. Neodymium sulfate was selectively recovered as crystals, and evaluated by chemical and crystallographic analyses. The findings presented in this investigation suggest that neodymium could be recovered from scrap magnet using an eco-friendly leaching methodology assisted by ammonium persulfate.

Keywords: Scrap magnet, persulfate, neodymium recovery, e-waste, leaching.

1. INTRODUCTION

In the rare-earth elements (REE) industry, around 36% of the world reserves are in China. Since the last three decades, this country has become the first mineral supplier with more than 90% of the REE international market (Abhilash et al., 2016; Meshram et al., 2016). This situation has promoted an imbalanced relationship between purchase requests and available REE in Chinese ore deposits (Binnemans and Jones, 2015). As a consequence, strict regulations have been adopted representing supply problems from primary sources. In order to promote suitable streams of REE without potential environmental risks, new alternatives are being studied around the recovery of REE from secondary sources (Sun et al., 2016).

One of the most important secondary sources is electronic waste (e-waste) (Gutiérrez-Gutiérrez et al., 2015). Large amounts of e-waste are annually collected owing to accelerated manufacture

and consumption of electronic devices as computers (PC), audio-visual and communication equipment (Akcil et al., 2015; Kaya, 2016). In the United States of America, a rough production of 34 million tons of e-waste was estimated in 2010, increasing these amounts until almost 50 million tons for 2018 and expecting a growth rate of 5% for the next years (Baldé et al., 2015). The excessive growth of these materials in landfills has been associated with rapid obsolescence of devices, which illustrates new models manufacture and their short lifespans (Habib Al Razi, 2016). Hence, e-waste could be proposed as a promising and plentiful secondary source to be treated by recycling processes.

Recently, Several investigations have proposed e-waste as a potential chain of supply to recover strategic metals for the development of low-carbon technologies (Binnemans et al., 2013; Ueberschaar and Rotter, 2015). Indeed, it has been revealed that significant fractions of these wastes are composed of scrap computers. These scraps contain Hard Disk Drivers (HDD), which are manufactured with diverse kinds of elements to carry out their performance. Those elements include transition (Cu, Ni, Fe), precious metals (Au, Ag, Pt) and REE (Dy, Nd). One of the most important constituents of HDD is Nd-Fe-B magnets. These magnets contain large amounts of Nd (15 – 30%), as well as other metals as Fe (70 – 60%) and Co (0 – 10%). Therefore, Nd-Fe-B magnets are suitable secondary sources to recover neodymium from scrap computers (Lixandru et al., 2017; Ueberschaar and Rotter, 2015).

The neodymium recovery from scrap computers has been suggested as a promising solution for decreasing the current shortage issues; however, the extraction treatments show real challenges that require proper approaches. Traditional disposal treatments such as incineration, landfill, and hydrometallurgy have been implemented to recycle e-waste, exhibiting in most of the cases some adverse effects on human health and environment (Kaya, 2016). On the one hand, incineration and landfill deteriorate the quality of ecosystems due to the emission of toxic vapors and the generation of hazardous by-products that are finally disposed into soils, freshwater and oceans (Hong et al., 2015; Woo et al., 2016). These treatments still take place in some developed countries and the majority of the developing ones. On the other hand, previous investigations have used conventional hydrometallurgical methods to recover neodymium from magnets in discarded HDD (Lixandru et al., 2017; Önal et al., 2017a). These methodologies have been developed by using strong acids solutions (e.g., HNO_3, HCl and H_2SO_4) in order to achieve the total dissolution of the metallic fraction (Ferron and Henry, 2015). Strong acids solutions could cause a negative environmental impact and strict chemical management of the generated by-products are required.

Conventional hydrometallurgy leaching process for neodymium recovery employes subsequent separation/purification stages. The precipitation separates neodymium from the leach solution generating double neodymium sulfate salts ($Nd_2(SO_4)_3 \cdot M_2SO_4 \cdot 6H_2O$ (M= NH_4, Na and K)). These salts are produced after pH adjustment with the addition of alkaline agents (NaOH, KOH, NH_3, etc.) (Lee et al., 2013; Lyman and Palmer, 1993). Organic collectors that form insoluble compounds are also used in the precipitation process (Panda et al., 2016; Vander Hoogerstraete et al., 2014; Yoon et al., 2016). Moreover, the precipitation process of neodymium sulfate generates compounds that require to be purified. This is the case of mechanical methods as filtration and centrifugation, which separate the soluble species and produce sediments of heterogeneous mixtures. For instance, Lyman and Palmer used filtration to reach the total Nd recovery as solid NdF_3 after hydrofluoric acid washes (Lyman and Palmer, 1993). While REE solids separation from liquor was carried out by using filtration, washing and centrifugation procedures also has been used (Vander Hoogerstraete et al., 2014). Although the high efficiency of these conventional methods seems to be a common characteristic, environmental concerns have increased on irreparable damages into ecosystems such as spillages risks, generation of toxic gases, insecure high concentrations, and untreatable complex hazardous by-products (Baral et al., 2014; Behera and Parhi, 2016; Robinson, 2009). Therefore, novel methodologies to recover neodymium using green reagents with lower environmental impact are being considered as one of the most important

goals to be achieved in recent years.

Nowadays, alternative methodologies with low environmental impact have been implemented to recover neodymium from scrap magnet. These methodologies include the use of phosphoric, ascorbic and acetic acid, which could reach short-time reactions with high and selective rates of recovery. In this sense, phosphoric and ascorbic acid solutions leached 99% of Nd at room temperature. After Nd leaching, $NdPO_4$ amorphous precipitates with minority Fe traces were obtained and recovered (Onoda and Nakamura, 2014). Meanwhile, similar neodymium recoveries were reached at optimum leaching conditions in acetic acid systems (CH_3COOH). In the mentioned system, ground scrap magnet (106 – 150 µm) was dissolved employing low concentrations of CH_3COOH (0.4 M), constant heating (80 °C) and stirring assistance during 4 h (Behera and Parhi, 2016).

Additionally, an eco-friendly alternative to recover metals from e-waste is also exhibited by persulfate salts. These salts show high oxidative sulfate radical ($SO_4^{\cdot-}$) speciation in water from the persulfate ions ($S_2O_8^{2-}$), where the formed radical suffers unlikely biological adsorption or deposition into sediments, seaweeds and animal life. These salts show high oxidative sulfate radical ($SO_4^{\cdot-}$) speciation in water from the persulfate ions ($S_2O_8^{2-}$), where the formed radical suffers unlikely biological adsorption or deposition into sediments, seaweeds and animal life (Alzate et al., 2017, 2016). Ammonium persulfate ($(NH_4)_2S_2O_8$) has shown several advantages compared to other persulfate salts such as high redox potential (2.08V vs. NHE), high solubility at 25 °C (850 g/L) and activation energies between 100 and 116 kJ mol^{-1} (Hassan et al., 2017; Matzek and Carter, 2016; PeroxyChem, 2017). The speciation from $(NH_4)_2S_2O_8$ to anion $S_2O_8^{2-}$ in aqueous solution also permits the thermal activation by producing $SO_4^{\cdot-}$ radicals that show high reduction potential (E^o= 2.5 – 3.1 V) at neutral pH (Sharma et al., 2015). Furthermore, it has been demonstrated that $(NH_4)_2S_2O_8$ could recover valuable metals without generation of harmful by-products. These by-products are compounds rich in metallic sulfates that have been employed in subsequent industrial processes without negative effects on the environment (Hyk and Kitka, 2017; Sharma et al., 2015).

Although $(NH_4)_2S_2O_8$ has been successfully used to recover valuable metals from e-waste, there has not been a single precedent in the literature on neodymium recovery from Nd-Fe-B magnet using $(NH_4)_2S_2O_8$ solutions (Alzate et al., 2017, 2016; Hyk and Kitka, 2017; Lu and Xu, 2017). In our previous work, we developed an eco-friendly process to selectively recover gold using $(NH_4)_2S_2O_8$ solutions. In this research Fe, Ni and Cu layers were partially oxidized, while gold was recovered in a solid state by peeling it from the substrate (Alzate et al., 2016). Furthermore, the obtained solid by-product composed of double ammonium sulfate salts were demonstrated to be harmless (Alzate et al., 2017, 2016). Statistical analyses from this investigation determined the experimental levels of the ammonium persulfate concentration and liquid/solid (L/S) ratio, as well as the numerical decrease of experimental assays due to optimization methodologies. These conditions were used in the present work as a starting point to select experimental levels of concentration, L/S ratio and temperature for the neodymium recovery by using $(NH_4)_2S_2O_8$. Additionally, temperature levels were further established following the thermal studies proposed by Yoon et al. (Yoon et al., 2014).

In this study, an environmentally-friendly method to recover neodymium from Nd-Fe-B magnet scrap using $(NH_4)_2S_2O_8$ was developed. A statistical analysis was performed to evaluate the influence of experimental parameters on the metal leaching and neodymium recovery. The established leaching conditions recovered neodymium as hydrated neodymium sulfate ($Nd_2(SO_4)_3.nH_2O$) and produced a mixture of metallic sulfates as by-products. The findings presented in this work showed a novel oxidative methodology to recover neodymium from Nd-Fe-B magnets and generate solid by-products without negative effects on the environment.

2. EXPERIMENTAL

2.1 Materials and characterization

The Nd–Fe–B magnets from end-of-life Hard Disk Drives (HDD) were provided by a local recycling company. The starting magnetic scrap was manually dismantled to separate non- metallic fraction from magnets. Thus, the dismantling of obsolete HDD gave as a result the collection of around 95% of the first magnetic scrap that was composed by Nd-Fe-B magnets attached to steel plates. A bulk sample of these classified magnets was demagnetized by heating at 400 °C for 45 min into a semi-industrial furnace (195 dm^3 inner volume). Figure 1 presents one sample of demagnetized magnets that were randomly selected due to its different size and shape. The separation showed a 26% ± 1.3 and 74% ± 1.1 of Nd-Fe-B magnets (Figure 1) and remaining steel plates, respectively.

Representative samples of magnets were then subjected to crushing stages in a type 3.5-cm upper-opening roll crusher (Consolidate Sturtevant Mill). After size reduction, the obtained powders were analyzed using X-Ray Fluorescence spectroscopy (XRF, ARL Optim'x). Further, additional evaluations were performed using scanning electron microscopy with energy dispersive X-ray spectroscopy (SEM-EDS, JEOL JSM-6490LV).

The leach solution was analyzed by microwave plasma atomic emission spectroscopy (MP-AES, AGILENT MP 4100) to quantify base metals (Fe, Co and Ni). After this characterization, the precipitation process was carried out, and the obtained neodymium sulfate was evaluated by X-Ray Fluorescence spectroscopy (XRF, ARL Optim'x), and X-Ray Diffraction (XRD, PANalytical-Empyrean) with Cu kα radiation (λ =1.5 Å) at 45 kV and 40 mA determined the crystallographic patterns. These patterns were evaluated with a slow 2θ step size and the angle range between 10° and 50°. The identification of the obtained diffraction patterns was assessed using High Score Plus software, crystallography Open Database (COD) and International Centre for Diffraction Data (ICDD). Finally, metallurgical indexes of the base metals were calculated between their initial amount in the sample and the final amount found in the solutions. Additionally, the formation of sulfate ions (SO_4^{2-}) into those leaching solutions was studied using ion chromatography with chemical suppression of eluent conductivity (IC, DIONEX ICS 1000).

Additionally, macro and microscopical analysis were performed using a stereomicroscope (AmScope SM-1TS-114S-10M) and SEM-EDS respectively.

Figure 1. Sample of demagnetized Nd-Fe-B magnet.

2.2 Leaching of magnetic scrap

The leaching of the ground sample was carried out employing ammonium persulfate (≥98% $(NH_4)_2S_2O_8$) as leaching agent at two concentrations (0.7 - 1.3 M). The solutions were prepared into glass reactors with a standard volume of 400 mL. Distilled water and mechanical stirring (400 rpm) were employed to prepare oxidative solutions with a L/S ratio of 25 and 50 mL/g at two different temperatures (25 ºC and 75 °C). These factors and levels were selected following the optimized results previously obtained by Alzate et al. (2016), whereas temperature levels were chosen due to the significant influence of temperature on the neodymium leaching kinetics (Yoon et al., 2014).

The selected samples of the ground Nd-Fe-B magnets were put into the leaching solutions for 15 minutes to evaluate the effect of experimental conditions on the leaching process. Furthermore, Medusa software and HSC chemistry software were used to calculate equilibrium constants and design a potential (Eh) vs. pH diagram (Pourbaix diagram) for the dissolved and solid species (HSC Chemistry Software, 2014, Medusa software, 2010). The Pourbaix diagram was employed to support the thermodynamic analysis of the aqueous system Fe-Nd-Co-Ni-SO_4^{2-} and illustrate the pH dependence on the selective formation of the neodymium sulfate. The used thermodynamic databases have been reported in previous investigations to study the lanthanides and actinides leaching (La, Nd, Ce, and Th) in PO_4-SO_4-H_2O systems (Kim and Osseo-Asare, 2012).

2.3 Recovery and analysis of neodymium sulfate

The leach solution at optimum conditions was used to selectively precipitate neodymium sulfate. The precipitation process was performed controlling pH at 0.1 and temperature at 75 °C to generate crystals of neodymium sulfate ($Nd_2(SO_4)_3.nH_2O$; n=3,5,7). The recovery of neodymium was carried out by following the optimal conditions achieved in the leaching process. In this recovery stage, the obtained solution was put into a glass reactor to selectively obtain solid crystals of neodymium sulfate by fractional precipitation. The precipitation reactions are ruled by the thermodynamic parameters, where negative values of ΔG^0 define the spontaneous shift in the direction of product formation. There is a major spontaneity to form neodymium sulfate at 75 °C ($\Delta G^0_{(75\ °C)}$ = -138.7 kJ/mol) than a lower temperature ($\Delta G^0_{(25\ °C)}$ = -111.1 kJ/mol). Thus, the neodymium recovery as neodymium sulfate is also influenced by increasing of temperature. These findings are in agreement with results previously published by Kim and Osseo-Asare in 2012, where it is described the effect of temperature and acidic environment on the recovery of neodymium sulfate (Kim and Osseo-Asare, 2012). The crystals of neodymium sulfate were purified and stabilized, whereas the remaining leach solution was unselectively precipitated to produce a solid mix of sulfates as by-products. Finally, the obtained neodymium sulfate and by-products were characterized by morphological, chemical and crystallographic techniques using methodology mentioned above.

2.4 Experimental design

In the present investigation, a full factorial 2^3 design was selected to evaluate the influence of three independent factors at two different levels on the Nd-Fe-B magnets leaching. The three independent factors (ammonium persulfate concentration, temperature, and L/S ratio) with their respective coded levels (low and high) are shown in Table 1. This full factorial 2^3 design employed eight experimental runs and one replicate to calculate the experimental error. A total of sixteen-

experimental runs was randomly performed to minimize interferences of unknown factors and secure the independence assumption among the value of factors.

Table 1. Levels of independent factors in full factorial 2^3 design.

Factors	**Levels**	
	Low (-1)	High (+1)
A: $[(NH_4)_2S_2O_8]$ (M)	0.7	1.3
B: Temperature (°C)	25	75
C: Liquid/Solid ratio (mL/g)	25	50

The significance of linear effects (A, B and C) on the response was statistically evaluated using analysis of variance (ANOVA) to accept the null hypothesis of the experiments. The calculated p-values with a significance level of 95% (α=0.05) were compared to evaluate the statistical effect of the studied factors on the leaching of Nd-Fe-B magnets. All the experimental data were analyzed by Design Expert software (Design Expert, 2015). This software also allowed to calculate a polynomial regression model of these data. The regression model that represents the full factorial design was explained by a first order equation (Eq. 1). In Eq.1, y is the leaching percentage of Nd-Fe-B magnets, x_1, x_2, x_3 are the coded factors, β_o comprises the global mean, β_1, β_2, β_3 are coefficients of the linear factors, β_{12}, β_{13}, β_{23} and β_{123} correspond with coefficients of the double and triple interactions respectively, and ε_{123} is pure error of the model.

$$y = \beta_o + \beta_1 x_1 + \beta_2 x_2 + \beta_3 x_3 + \beta_{12} x_1 x_2 + \beta_{13} x_1 x_3 + \beta_{23} x_2 x_3 + \beta_{123} x_1 x_2 x_3 + \varepsilon_{123} \quad (1)$$

3. RESULTS AND DISCUSSION

3.1 Characterization

The Nd-Fe-B magnets fraction was ground and subjected to particle size reduction analysis. The size reduction showed a 70% of powders with sizes less than 420 µm, irregular morphologies and a local composition were associated with Fe (67.2 wt%), and Nd (32.8 wt%) (Figure 2a and Figure 2b). These powders were also evaluated by XRF in order to reach representative measurement, and the results showed contents of neodymium (31.4 wt%) and iron (64.8 wt%) as described in Table 2. It can be seen that both analyses of chemical composition agreed. Additionally, it was also found other metals in minor amounts, such as cobalt, nickel, aluminium and copper. These results are in agreement with those presented by Önal et al (Önal et al., 2015). Other works have reported the composition of boron lower to 1%wt. indicating a negligent effect on the subsequent processes of leaching and recovery ((Behera and Parhi, 2016; Önal et al., 2017b, 2015)); based on this, the presence of this metalloid was ignored in this investigation.

Table 2. Chemical composition of the ground Nd-Fe-B magnets.

Elements (wt%)	Fe	Nd	Co	Ni	Al	Cu	B	Others
	64.8	31.4	1.9	0.6	0.4	0.2	-	0.7
(Önal et al., 2015)	65.0	22.4	1.05	0.6	0.4	0.2	0.8	9.3

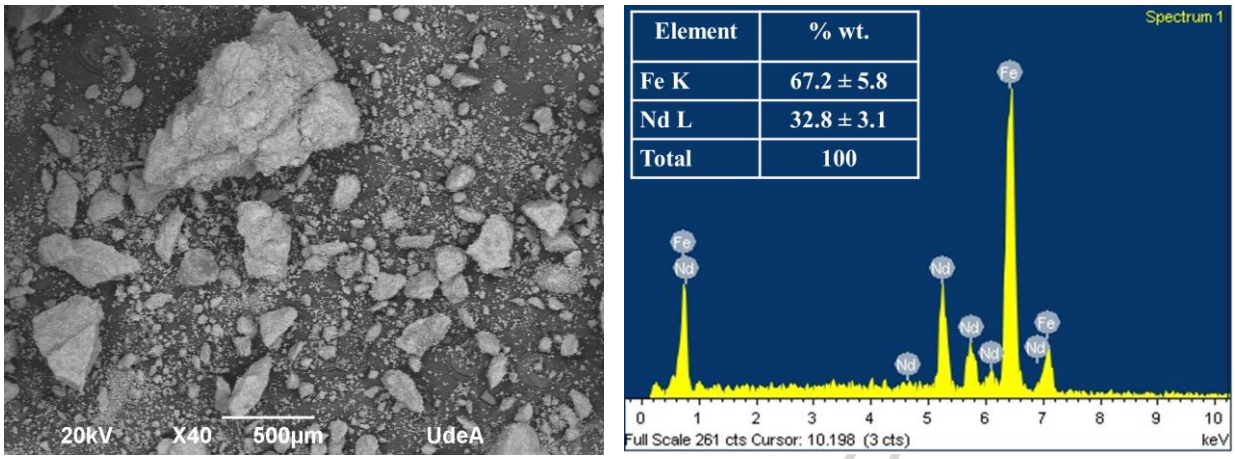

(a) (b)

Figure 2. SEM (a) and EDS (b) analysis of the ground Nd-Fe-B magnets.

3.2 Redox and solubility equilibria

The leaching of the ground sample of Nd-Fe-B magnets was modeled by designing an Eh vs. pH diagram (Pourbaix diagram) for dissolved and solid species individually formed (Figure 3). The designed potential-pH diagram was conducted using the proposed experimental values of concentration and temperature (75 °C) to obtain an accurate understanding of redox behavior for the samples in the aqueous system Fe-Nd-Co-Ni-SO_4^{2-}. Table 3 shows thermodynamical constants for the leaching reactions. The Pourbaix diagram for this system showed the coexistence of Nd and Fe species at a low pH value (pH < 4) (Eq. 2 - 3). While aqueous species of iron (Fe^{2+}) remained in solution at oxidative potential values, Nd was transformed into a soluble sulfate and then in a thermodynamically stable neodymium sulfate octahydrate solid as shown in Table 3 and Eq. 6. A similar result was shown by iron with the formation of iron sulfate heptahydrate in a pH range between 3.8 and 6.5 (Table 3, Eq. 7), whereas oxidized Co^{2+} ions also could remain in this state until pH < 6.9 (Table 3, Eq. 4) and become $Co(OH)_2$ at higher alkaline conditions. Although nickel (Table 3, Eq. 5) and other metals also suffered an oxidative process, it was not possible to represent a suitable stability region due to the low concentration of these metals in the experimental leach solution.

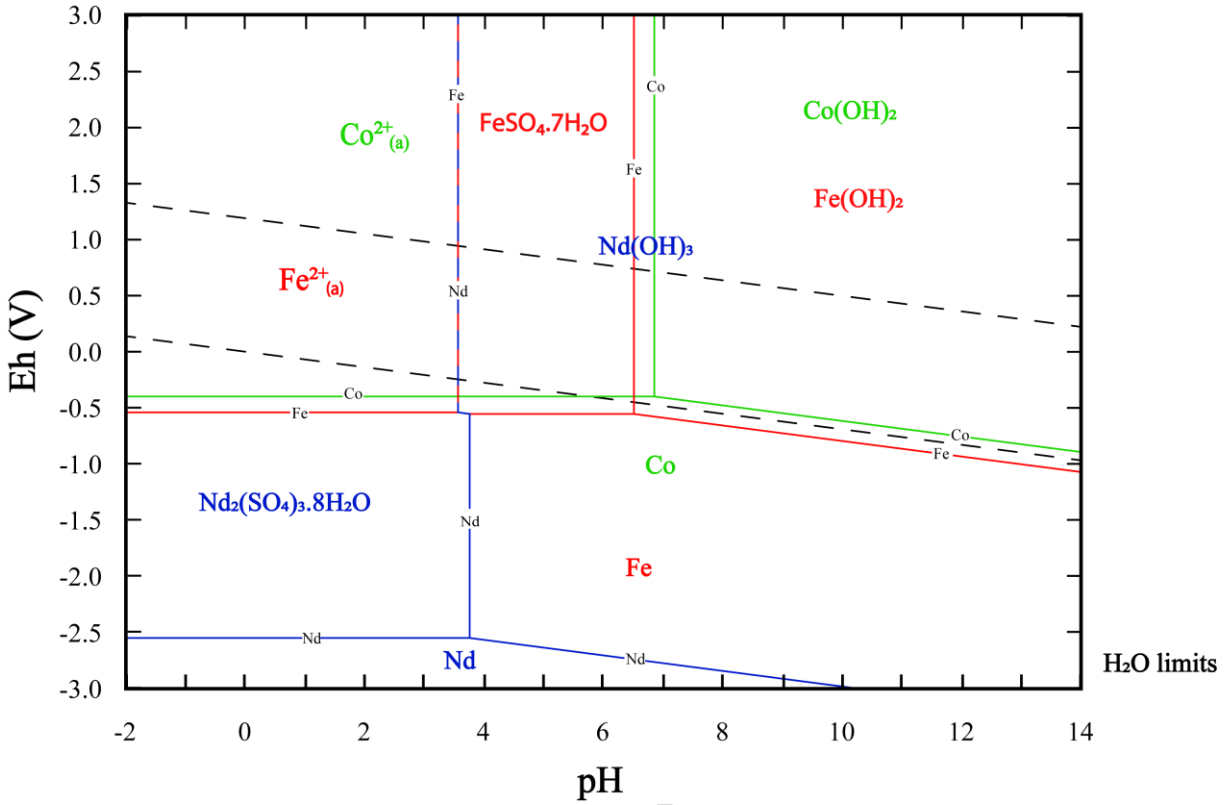

Figure 3. Eh–pH diagram for Fe–Nd–Co–Ni–SO_4^{2-}–H_2O system at 75 °C with [Fe]: $1.2x10^{-2}$ M, [Nd]: $2.1x10^{-3}$ M, [Co]: $3.1x10^{-4}$ M, [Ni]: $1.1x10^{-4}$ M, $[(NH_4)_2S_2O_8]$: 1.3 M.

Table 3. Thermodynamic constants for the leaching reactions.

Equation	Redox reaction	Redox potential (E°)	Log $K_{(75\,°C)}$
(2)	$Nd \leftrightarrow Nd^{3+}_{(a)} + 3e^-$	-2.3	-
(3)	$Fe \leftrightarrow Fe^{2+}_{(a)} + 2e^-$	-0.4	-
(4)	$Co \leftrightarrow Co^{2+}_{(a)} + 2e^-$	-0.2	-
(5)	$Ni \leftrightarrow Ni^{2+}_{(a)} + 2e^-$	-0.2	-
(6)	$2Nd^{3+} + 3SO_4^{2-}_{(a)} + 8H_2O \leftrightarrow Nd_2(SO_4)_3.8H_2O_{(s)}$	-	20.8
(7)	$Fe^{2+} + SO_4^{2-}_{(a)} + 7H_2O \leftrightarrow FeSO_4.7H_2O$	-	2.4
(8)	$S_2O_8^{2-} + 2e^- \leftrightarrow 2SO_4^{2-}$	1.8 - 2.7	-
(9)	$Nd^{3+} + 2\,SO_4^{2-} \leftrightarrow 2Nd(SO_4)_2^-$	-	5.7
(10)	$Nd^{3+} + SO_4^{2-} \leftrightarrow 2NdSO_4^+$	-	4.2
(11)	$Fe^{2+} + SO_4^{2-}_{(a)} \leftrightarrow FeSO_{4(a)}$	-	3.2
(12)	$Ni^{2+} + SO_4^{2-}_{(a)} \leftrightarrow NiSO_{4(a)}$	-	2.8
(13)	$Co^{2+} + SO_4^{2-}_{(a)} \leftrightarrow CoSO_{4(a)}$	-	2.7

3.3 Leaching results

Table 4 shows the experimental design layout. Leaching of Fe, Co and Ni was considered as secondary responses that permitted the calculation of the neodymium sulfate formation. After the sixteen experimental runs were performed, the standard deviation of the main response (Leaching of Nd-Fe-B magnets) was determined to be ≤ 0.23%. In Table 4, the maximum leaching of Nd-Fe-

B magnets (98.6% ± 0.1) was observed around 15 minutes. This leaching rate reached the highest conditions of linear factors in the actual levels (+1, +1, +1). The significance of these factors and their interactions were studied by analysis of variance (ANOVA) (Table 5). The ANOVA showed p-values lower than the significance level ($\alpha = 0.05$) for all the linear factors and interactions, indicating that $(NH_4)_2S_2O_8$ concentration, L/S ratio and temperature vary together in their effect on the response.

Once the analysis of variance was performed, Design Expert software calculated a mathematical regression model to explain the leaching of Nd-Fe-B magnets. Equation 8 shows the fitted model. Further, the coefficient of determination ($R^2 = 0.9997$) demonstrated the validity of the model. In concordance with this result, predicted R^2 (Pred-$R^2 = 0.9987$) and adjusted R^2 (Adj-$R^2 = 0.9995$) were in suitable agreement given that their difference was lower than 0.2 value.

$$\%\text{Leaching}_{\text{Nd-Fe-Bmagnets}} = 70.03+5.42A+16.20B+2.08C+1.32AB+1.92AC+1.39BC+0.27ABC + 0.05 \quad (8)$$

Equation 8 exhibts that A, B and C has a positive sign which indicates a direct influence of $(NH_4)_2S_2O_8$ concentration, temperature, L/S ratio on the leaching of magnets. Factor B was the most influential linear factor. This could be explained by the acceleration of leaching by increasing temperature. Leaching efficiency of Nd-Fe-B magnets reached greater than 98% at the highest value of temperature (Table 4, exp 15-16). The leaching process reached the maximum redox potential value for the couple $S_2O_8^{2-}/SO_4^{\cdot-}$ (Table 3, Eq. 8) with the activation of persulfate by temperature assistance (Sharma et al., 2015). This thermal activation caused a strong oxidative reaction that permitted to dissolve the metallic fraction with the formation of two $SO_4^{\cdot-}$ radicals ($S_2O_8^{2-}$ + heat → 2 $SO_4^{\cdot-}$). In this sense, the formation of sulfate free radicals has widely been proved by heat exposition given as result a energetic reaction and the subsequent leaching of metals (Alzate et al., 2017; Chen et al., 2017; Hyk and Kitka, 2017; Matzek and Carter, 2017; Sharma et al., 2015).

The high oxidative potential indicates the preferential leaching over Nd/Nd^{3+} followed by the leaching of the Fe/Fe^{2+}, Co/Co^{2+} and Ni/Ni^{2+} as can be seen in Table 3 (Eq. 2 - 5) (Prakash et al., 2014). Meanwhile, the positive effect of A and C factors on the response could be attributed to the proper availability of aqueous media to guarantee the interaction between the sample of Nd-Fe-B magnets and the formed oxidative $SO_4^{\cdot-}$. Furthermore, the contribution of all the interactions was positive showing similar relevance.

The oxidative reaction of this agent combined with temperature indicated leaching of metals around 98% with a reaction time of 15 min. After the leaching process, the leach solution acquired a pink color indicating a stepwise reaction for the neodymium sulfate formation at pH 0.1. In this study, soluble intermediates complexes ($NdSO_4^+$, $Nd(SO_4)_2^-$) could be formed during the leaching process. The formation of these complexes showed a dependence on temperature and concentration of neodymium and sulfate ions as previously indicated by several authors (Kim and Osseo-Asare, 2012; Migdisov et al., 2006). The complex $Nd(SO_4)_2^-$ exhibited an equilibrium constant higher than that of the $NdSO_4^+$ (Table 3, Eq. 9 - 10), indicating that the former complex has a preferential formation under the established parameters of temperature and pH (75 °C, pH 0.1) prior to obtaining of $Nd_2(SO_4)_3.8H_2O$. However, when over-saturated sulfate solutions (> $1x10^{-2}$ M) are used, the thermodynamic stability is controlled by $Nd_2(SO_4)_3.8H_2O$. This has been evident in the Pourbaix diagrams proposed by (Kim and Osseo-Asare, 2012), where the soluble $Nd_2(SO_4)_3.8H_2O$ shows a predominance in acidic solutions (pH< 4.0) (Kim and Osseo-Asare, 2012). Finally, the increase in temperature leads to form the solid $Nd_2(SO_4)_3.8H_2O_{(s)}$ from the solution due to its low solubility.

In contrast, the remaining soluble sulfates of iron ($FeSO_{4(a)}$), nickel ($NiSO_{4(a)}$) and cobalt ($CoSO_{4(a)}$) were also formed at pH of 0.1 and 75 °C (Table 3, Eq. 11 - 13), showing an unlikely

interference on the stability of the formed neodymium complexes. According to this, the equilibrium constants greater than zero for the metallic sulfates exhibited a preferential behavior of stability such as Nd>Fe>Ni>Co. The absence of this interference could be observed in both the current Eh-pH diagram at 75 °C (Figure 3) and the experimental results presented in this investigation.

Table 4. Experimental design with factors and response values for the Nd-Fe-B magnet leaching.

Experiment	Factors and levels			% Leaching over 15 min			
Run	A	B	C	Base metal			Nd-Fe-B Magnets
	$[(NH_4)_2S_2O_8]$ (M)	T (°C)	L/S ratio (mL/g)	Fe	Co	Ni	
1-2	0.7	25	25	35.4±1.6	8.9±0.1	2.5±0.4	55.6±0.1
3-4	1.3	25	25	51.2±0.7	30.3±1.2	3.9±0.1	55.6±0.4
5-6	0.7	75	25	66.6±1.2	45.6±0.6	6.2±0.5	78.2±0.1
7-8	1.3	75	25	73.8±0.4	54.7±1.2	4.8±0.6	87.3±0.2
9-10	0.7	25	50	90.7±0.9	78.1±0.2	5.3±0.4	48.8±0.3
11-12	1.3	25	50	91.8±1.4	76.4±0.3	5.7±0.2	60.2±0.1
13-14	0.7	75	50	68.4±0.4	40.8±1.3	7.7±0.2	80.7±0.2
15-16	1.3	75	50	64.4±0.9	39.2±0.5	5.17±0.7	98.6±0.1

Table 5. Analysis of variance (ANOVA) for the magnet leaching.

Source	Sum of Squares	Degree of freedom	Mean Squares	p-value
Model	4858.1	7	694.0	< 0.0001
A- $[(NH_4)_2S_2O_8]$	470.4	1	470.4	< 0.0001
B- Temperature	4200.0	1	4200.0	< 0.0001
C- L/S Ratio	69.1	1	69.1	< 0.0001
AB	27.8	1	27.8	< 0.0001
AC	58.7	1	58.7	< 0.0001
BC	31.1	1	31.1	< 0.0001
ABC	1.1	1	1.1	0.00015
Pure Error	0.4	8	0.05	
Corrected Total	4858.5	15		

The current oxidative system dissolved the Nd-Fe-B magnet using the combination of the highest levels for concentration, temperature and L/S ratio. Hence, contour plots were generated to describe the simultaneous combination of the two factors on for the leaching of the Nd-Fe-B magnets, where the third factor was held at the highest level. Figures 4a-c show a wide red region where the leaching efficiency of magnets reached greater than 98% through the combination of $(NH_4)_2S_2O_8$ concentration at 1.3 M, a temperature of 75 °C and L/S ratio of 50 mL/g for a reaction time of 15 min.

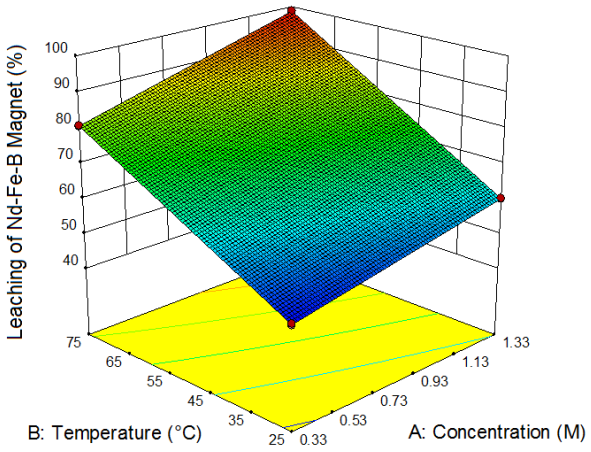

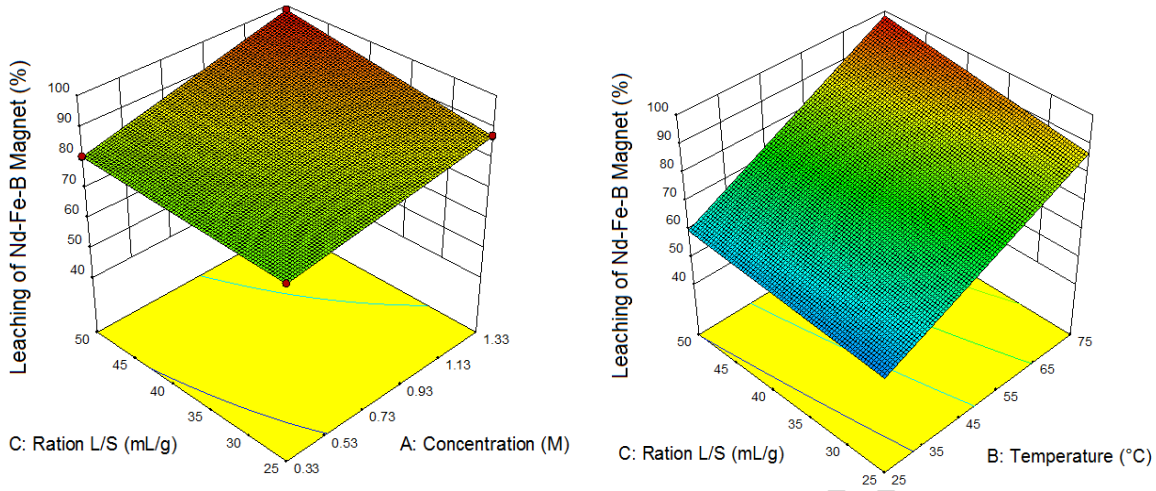

Figure 4. Leaching of the Nd-Fe-B magnets (a) A: $(NH_4)_2S_2O_8$] and B: Temperature with C= 50 mL/g, (b) A: [$(NH_4)_2S_2O_8$] and C: L/S ratio with B= 75 °C, (c) B: Temperature and C: L/S ratio with A= 1.3 M.

3.4 Precipitation and recovery of neodymium sulfate

Neodymium was recovered by controlling temperature and pH parameters of the leach solution, of which a selective separation of neodymium sulfate crystals occurred. After this separation, the obtained crystals were purified and they can be seen in Figure 5. At macroscopic scales, it is possible to observe the typical pink color of the neodymium sulfate crystals and its diverse morphologies. The SEM/EDS analysis was subsequently performed to evaluate the morphology at the microscopic level and chemical composition of crystals. Figure 6 indicates the selective precipitation thin rectangular prisms with similarities to a monoclinic crystalline structure. Based on the EDS results, the elementary composition showed neodymium sulfate without evidence of iron traces.

Figure 5. Crystals composed of neodymium sulfate.

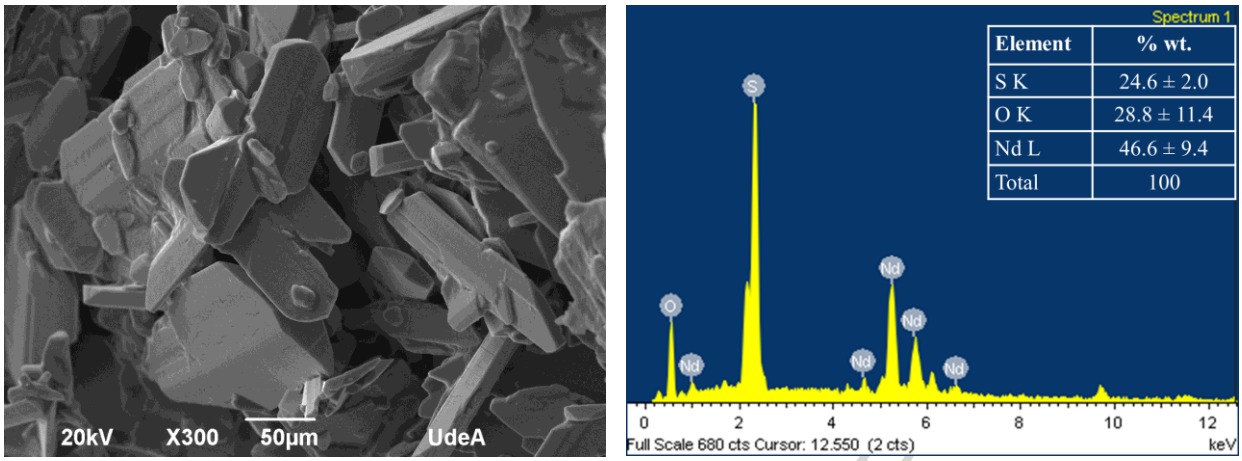

(a) (b)

Figure 6. SEM image (a) and EDS analysis (b) for $Nd_2(SO_4)_3$ crystals.

The XRD analysis exhibited crystallographic phases for the neodymium sulfate (Figure 7). These patterns showed correspondence with the crystallographic reference patterns of neodymium sulfate with diverse types of hydration ($Nd_2(SO_4)_3.nH_2O$, where n= 4,5 and 8). According to this result, the main peaks with the highest intensity were observed at 14.5°, 27.8° and 42.6°. Similarly, iron sulfate heptahydrate ($FeSO_4.7H_2O$) patterns were also determined in a reduced intensity for the pick at 27.7°. Although this recovery process has been reached with a large selectivity level, it is entirely reasonable to evaluate the iron participation with additional assessments. The crystallographic predominance of neodymium sulfate with minority iron phases agreed with the chemical composition represented in XRF results (Table 6). In this result, neodymium as oxide was the highest amount as target metal (23.5 %wt.) with minority iron and other traces. The presence of sulfate ions constituted three-quarters of the total composition because of the chemical nature of the leach solution. The purity of the generated neodymium sulfate was calculated by relating rare-earth oxides over the total metals in the absence of sulfate ions. This purity showed a value of 96% indicating a selective and effective recovery process of neodymium.

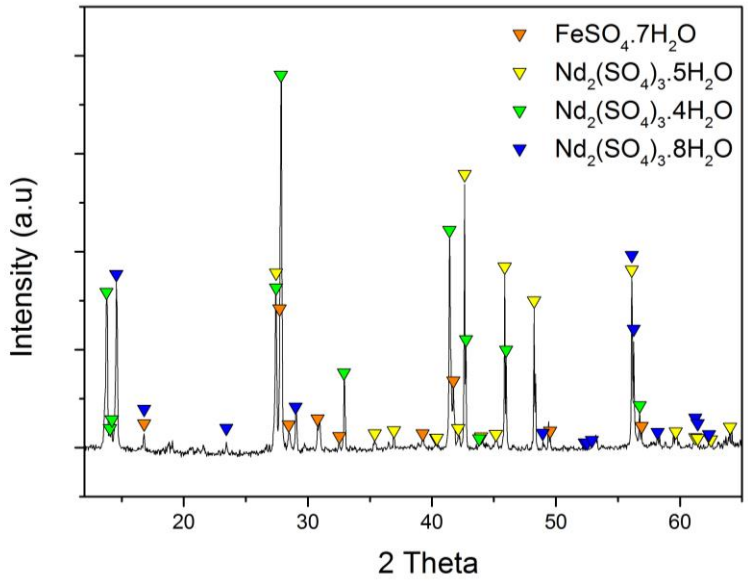

Figure 7. XRD pattern for the recovered hydrated $Nd_2(SO_4)_3$ crystals assisted under temperature and pH control.

Table 6. Chemical composition of the synthetized neodymium sulfate.

Composition (wt%)	SO_4^{2-}	Nd_2O_3	Fe_2O_3	Al_2O_3	Others
	75.5	23.5	0.8	0.1	<0.1

3.5 Evaluation of the obtained by-products after selective neodymium recovery

After the selective neodymium recovery, the resulting solution behaved following the Pourbaix diagram for Fe–Nd–Co–Ni–SO_4^{2-}–H_2O (Figure 3). These results indicated the formation of soluble hydrated iron sulfate at 75 °C and pH 0.1. Subsequently, a hydrated by-product of iron sulfate was generated by cooling precipitation; it means that the resulting solution was heated and rapidly cooled down. This obtained by-product with this precipitation process can be seen in Figure 8.a. In order to analyze crystallographic phases and chemical composition for the by-products, XRD and XRF tests were carried out. Firstly, the crystallographic phases for iron sulfate were associated with three and six hydrations ($FeSO_4.3H_2O$, $FeSO_4.6H_2O$) (Figure 8.b). Furthermore, other sulfates such as hydrated nickel and cobalt sulfates ($NiSO_4.2H_2O$, $CoSO_4.2H_2O$) were also determined. In the case of ammonium sulfate ($(NH_4)_2SO_4$), the XRD pattern showed that this compound could be formed after the reaction of dissociation of $(NH_4)_2S_2O_8$ in the neodymium recovery. In general, characteristic peaks with large intensity for $(NH_4)_2SO_4$ were observed at 17.8°, 23.5°, 26.2°, and 30.5°, while metallic sulfates were represented by hydrated iron, cobalt and nickel sulfates. Secondly, the absence of toxic or harmful compounds was exhibited after chemical composition analysis. These analyses suggested that the obtained by-products in the solid state do not represent an environmental hazard due to the contamination of iron, cobalt, and nickel sulfate (Table 7). Thus, the obtained by-products in the solid state show the absence of toxic or harmful salts. Furthermore, the amounts of metals could be eventually implemented as iron precursors for technological fields based on pigments and fertilizers (El-jendoubi et al., 2011; Tolinski, 2015; Xue et al., 2017).

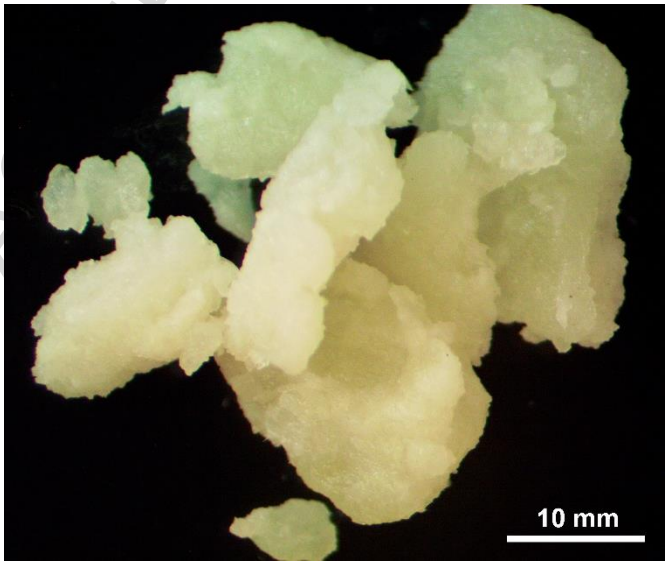

(a)

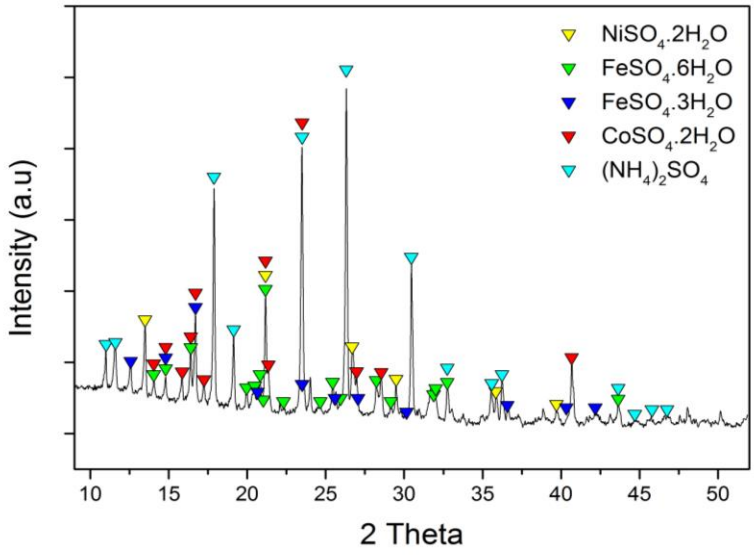

(b)

Figure 8. By-products image (a) and XRD pattern (b) obtained from the recovery process of neodymium sulfate assisted under temperature and pH control.

Table 7. Chemical composition for the obtained by-products.

Composition (wt%)	SO_4^{2-}	Fe	Co	Ni
	78.9	19.4	1.6	<0.1

4. CONCLUSIONS

The recovery of neodymium from scrap Nd-Fe-B magnets was developed using a novel eco-friendly alternative with ammonium persulfate. Optimal conditions were established as $(NH_4)_2S_2O_8$ concentration of 1.3 M, a temperature of 75 °C and L/S ratio of 50 mL/g. These conditions allowed 98% of neodymium recovery after 15 minutes of reaction time. The influence of concentration, temperature, and L/S ratio were statistically significant as well as the interaction between all the factors. In this regard, the temperature showed the highest influence on the scrap leaching and the subsequent neodymium recovery. This agreed with the thermodynamic behavior described in the aqueous Pourbaix diagram for Fe–Nd–Co–Ni–SO_4^{2-} system. Moreover, the calculated Gibbs free energy values showed the spontaneous shift in the direction of product formation. Based on those optimal experimental results, neodymium was recovered as crystals of neodymium sulfate using inverse solubility principles with temperature (75 °C) and pH (0.1) adjustments (Kim and Osseo-Asare, 2012). The chemical and crystallographical analysis confirmed the selective precipitation of neodymium sulfate with a high level of purity (96%) and minimal presence of other metal traces (>0.1 wt%). The findings of this investigation demonstrated for the first time a cleaner path to recover neodymium from scrap Nd-Fe-B magnet using ammonium persulfate. The implementation of this methodology exhibits a close loop neodymium recycling process with high selectivity and non-environmental issues.

ACKNOWLEDGEMENTS

The authors would like to sincerely acknowledge the national fund for financing of science, technology and innovation (FRANCISCO JOSE DE CALDAS) (Project N_0 FP44842-591-2014) and the University of Antioquia sustainability strategy (2014-2015) for the financial support to successfully develop this research. The authors would also like to thank the Colombian companies INSUMON S.A.S and LITO S.A.S for providing samples, staff and facilities for the experimental tests.

REFERENCES

Abhilash, S.S., Meshram, P., Pandey, B.D., 2016. Metallurgical processes for the recovery and recycling of lanthanum from various resources - A review. Hydrometallurgy 160, 47–59. https://doi.org/10.1016/j.hydromet.2015.12.004

Akcil, A., Erust, C., Gahan, C.S., Ozgun, M., Sahin, M., Tuncuk, A., 2015. Precious metal recovery from waste printed circuit boards using cyanide and non-cyanide lixiviants - A review. Waste Manag. 45, 258–271. https://doi.org/10.1016/j.wasman.2015.01.017

Alzate, A., López, E., Serna, C., Gonzalez, O., 2017. Gold recovery from printed circuit boards by selective breaking of internal metallic bonds using activated persulfate solutions. J. Clean. Prod. 166, 1102–1112. https://doi.org/10.1016/j.jclepro.2017.08.124

Alzate, A., López, M.E., Serna, C., 2016. Recovery of gold from waste electrical and electronic equipment (WEEE) using ammonium persulfate. Waste Manag. 57, 113–120. https://doi.org/10.1016/j.wasman.2016.01.043

Baldé, C.P., Wang, F., Kuehr, R., Huisman, J., 2015. The Global E-waste Monitor 2014: Quantities, Flows and Resources, The global e-waste monitor – 2014. IAS – SCYCLE, Bonn, Germany. https://doi.org/9789280845556

Baral, S.S., Shekar, K.R., Sharma, M., Rao, P. V., 2014. Optimization of leaching parameters for the extraction of rare earth metal using decision making method. Hydrometallurgy 143, 60–67. https://doi.org/10.1016/j.hydromet.2014.01.006

Behera, S.S., Parhi, P.K., 2016. Leaching kinetics study of neodymium from the scrap magnet using acetic acid. Sep. Purif. Technol. 160, 59–66. https://doi.org/10.1016/j.seppur.2016.01.014

Binnemans, K., Jones, P.T., 2015. Rare Earths and the Balance Problem. J. Sustain. Metall. 1, 29–38. https://doi.org/10.1007/s40831-014-0005-1

Binnemans, K., Jones, P.T., Blanpain, B., Van Gerven, T., Yang, Y., Walton, A., Buchert, M., 2013. Recycling of rare earths: a critical review. J. Clean. Prod. 51, 1–22. https://doi.org/10.1016/j.jclepro.2012.12.037

Chen, Y., Deng, P., Xie, P., Shang, R., Wang, Z., Wang, S., 2017. Chemosphere Heat-activated persulfate oxidation of methyl- and ethyl-parabens : Effect , kinetics , and mechanism. Chemosphere 168, 1628–1636. https://doi.org/10.1016/j.chemosphere.2016.11.143

Design Expert, 2015. Design Expert (No. Version 9.0.4.1. Stat-Ease). Stat-Ease Inc, 2021 East Hennepin Ave, Suite 480, Minneapolis, MN 55413.

Ferron, C.J., Henry, P., 2015. A review of the recycling of rare earth metals. Can. Metall. Q. 54, 388–394. https://doi.org/10.1179/1879139515Y.0000000023

Gutiérrez-Gutiérrez, S.C., Coulon, F., Jiang, Y., Wagland, S., 2015. Rare earth elements and critical metal content of extracted landfilled material and potential recovery opportunities. Waste Manag. 42, 128–136. https://doi.org/10.1016/j.wasman.2015.04.024

Habib Al Razi, K.M., 2016. Resourceful recycling process of waste desktop computers: A review study. Resour. Conserv. Recycl. 110, 30–47. https://doi.org/10.1016/j.resconrec.2016.03.017

Hassan, M., Wang, X., Wang, F., Wu, D., Hussain, A., Xie, B., 2017. Coupling ARB-based biological and photochemical (UV / TiO 2 and UV / S 2 O 2 8) techniques to deal with sanitary landfill leachate. Waste Manag. 63, 292–298. https://doi.org/10.1016/j.wasman.2016.09.003

Hong, J., Shi, W., Wang, Y., Chen, W., Li, X., 2015. Life cycle assessment of electronic waste treatment. Waste Manag. 38, 357–65. https://doi.org/10.1016/j.wasman.2014.12.022

Hyk, W., Kitka, K., 2017. Highly efficient and selective leaching of silver from electronic scrap in the base-activated persulfate – ammonia system. Waste Manag. 60, 601–608. https://doi.org/10.1016/j.wasman.2016.12.038

Kaya, M., 2016. Recovery of metals and nonmetals from electronic waste by physical and chemical recycling processes. Waste Manag. 57, 64–90. https://doi.org/10.1016/j.wasman.2016.08.004

Kim, E., Osseo-Asare, K., 2012. Aqueous stability of thorium and rare earth metals in monazite hydrometallurgy: Eh-pH diagrams for the systems Th-, Ce-, La-, Nd- (PO 4)-(SO 4)-H 2O at 25 ºC. Hydrometallurgy 113–114, 67–78. https://doi.org/10.1016/j.hydromet.2011.12.007

Lee, C.-H., Chen, Y.-J., Liao, C.-H., Popuri, S.R., Tsai, S.-L., Hung, C.-E., 2013. Selective Leaching Process for Neodymium Recovery from Scrap Nd-Fe-B Magnet. Metall. Mater. Trans. A 44, 5825–5833. https://doi.org/10.1007/s11661-013-1924-3

Lixandru, A., Venkatesan, P., Jönsson, C., Poenaru, I., Hall, B., Yang, Y., Walton, A., Güth, K., Gauß, R., Gutfleisch, O., 2017. Identification and recovery of rare-earth permanent magnets from waste electrical and electronic equipment. Waste Manag. https://doi.org/10.1016/j.wasman.2017.07.028

Lu, Y., Xu, Z., 2017. Recycling non-leaching gold from gold-plated memory cards : Parameters optimization , experimental veri fi cation , and mechanism analysis. J. Clean. Prod. 162, 1518–1526. https://doi.org/http://dx.doi.org/10.1016/j.jclepro.2017.06.094

Lyman, J.W., Palmer, G.R., 1993. Recycling of Neodymium Iron Boron Magnet Scrap, 9481 Repor. ed. United States Department of Interior, Washington, D.C.

Matzek, L.W., Carter, K.E., 2017. Sustained persulfate activation using solid iron : Kinetics and application to ciprofloxacin degradation. Chem. Eng. J. 307, 650–660. https://doi.org/10.1016/j.cej.2016.08.126

Matzek, L.W., Carter, K.E., 2016. Activated persulfate for organic chemical degradation: A review. Chemosphere. https://doi.org/10.1016/j.chemosphere.2016.02.055

Meshram, P., Pandey, B.D., Mankhand, T.R., 2016. Process optimization and kinetics for leaching of rare earth metals from the spent Ni-metal hydride batteries. Waste Manag. 51, 196–203. https://doi.org/10.1016/j.wasman.2015.12.018

Migdisov, A.A., Reukov, V.V., Williams-Jones, A.E., 2006. A spectrophotometric study of neodymium(III) complexation in sulfate solutions at elevated temperatures. Geochim. Cosmochim. Acta 70, 983–992. https://doi.org/10.1016/j.gca.2005.11.001

Önal, M.A.R., Aktan, E., Borra, R.C., Blanpain, B., Gerven, T. Van, Guo, M., 2017a. Hydrometallurgy Recycling of NdFeB magnets using nitration, calcination and water leaching for REE recovery. Hydrometallurgy 167, 115–123. https://doi.org/10.1016/j.hydromet.2016.11.006

Önal, M.A.R., Borra, C.R., Guo, M., Blanpain, B., Gerven, T. Van, 2015. Recycling of NdFeB Magnets Using Sulfation, Selective Roasting, and Water Leaching. J. Sustain. Metall. 1, 199–215. https://doi.org/10.1007/s40831-015-0021-9

Önal, M.A.R., Borra, C.R., Guo, M., Blanpain, B., Van Gerven, T., 2017b. Hydrometallurgical recycling of NdFeB magnets: Complete leaching, iron removal and electrolysis. J. Rare Earths 35, 574–584. https://doi.org/10.1016/S1002-0721(17)60950-5

Onoda, H., Nakamura, R., 2014. Recovery of neodymium from an iron–neodymium solution using phosphoric acid. J. Environ. Chem. Eng. 2, 1186–1190. https://doi.org/10.1016/j.jece.2014.04.019

Panda, R., Jha, M.K., Hait, J., Kumar, G., Singh, R.J., Yoo, K., 2016. Extraction of lanthanum and neodymium from leach liquor containing rare earth metals (REMs). Hydrometallurgy 165, 106–110. https://doi.org/10.1016/j.hydromet.2015.10.019

PeroxyChem, 2017. Persulfates Technical information. PeroxyChem, Tonawanda, New York.

Prakash, V., Sun, Z.H.I., Sietsma, J., Yang, Y., 2014. Electrochemical recovery of rare earth elements from magnet scraps - a theoretical analysis, in: ERES2014: 1st European Rare Earth Resources Conference. ERES2014, The Netherlands, pp. 163–170.

Robinson, B.H., 2009. E-waste: An assessment of global production and environmental impacts. Sci. Total Environ. 408, 183–191. https://doi.org/10.1016/j.scitotenv.2009.09.044

Sharma, J., Mishra, I.M., Kumar, V., 2015. Degradation and mineralization of Bisphenol A (BPA) in aqueous solution using advanced oxidation processes: UV/H2O2 and UV/S2O2 oxidation systems. J. Environ. Manage. 156, 266–275. https://doi.org/10.1016/j.jenvman.2015.03.048

Sun, Z., Xiao, Y., Agterhuis, H., Sietsma, J., Yang, Y., 2016. Recycling of metals from urban mines - A strategic evaluation. J. Clean. Prod. 112, 2977–2987. https://doi.org/10.1016/j.jclepro.2015.10.116

Ueberschaar, M., Rotter, V.S., 2015. Enabling the recycling of rare earth elements through product design and trend analyses of hard disk drives. J. Mater. Cycles Waste Manag. 17, 266–281. https://doi.org/10.1007/s10163-014-0347-6

Vander Hoogerstraete, T., Blanpain, B., Van Gerven, T., Binnemans, K., 2014. From NdFeB magnets towards the rare-earth oxides: a recycling process consuming only oxalic acid. RSC Adv. 4, 64099–64111. https://doi.org/10.1039/C4RA13787F

Woo, S.H., Lee, D.S., Lim, S.R., 2016. Potential resource and toxicity impacts from metals in waste electronic devices. Integr. Environ. Assess. Manag. 12, 364–370. https://doi.org/10.1002/ieam.1710

Yoon, H.-S., Kim, C.-J., Chung, K.W., Lee, S.-J., Joe, A.-R., Shin, Y.-H., Lee, S.-I., Yoo, S.-J., Kim, J.-G., 2014. Leaching kinetics of neodymium in sulfuric acid from E-scrap of NdFeB permanent magnet. Korean J. Chem. Eng. 31, 706–711. https://doi.org/10.1007/s11814-013-0259-5

Yoon, H.S., Kim, C.J., Chung, K.W., Kim, S.D., Lee, J.Y., Kumar, J.R., 2016. Solvent extraction, separation and recovery of dysprosium (Dy) and neodymium (Nd) from aqueous solutions: Waste recycling strategies for permanent magnet processing. Hydrometallurgy 165, 27–43. https://doi.org/10.1016/j.hydromet.2016.01.028

HIGHLIGHTS

- Neodymium was recovered from scrap magnet using ammonium persulfate solutions
- Equilibrium phases for the persulfate system were analyzed by Eh vs pH diagram
- Persulfate ions speciated in sulfate radicals by increasing temperature
- Sulfate radicals leached Nd-Fe-B magnets and neodymium sulfate was recovered
- The produced solid by-products are eco-friendly.